Heliyon 9 (2023) e22030

Contents lists available at ScienceDirect

Heliyon

journal homepage: www.cell.com/heliyon

Heuristic computing with active set method for the nonlinear Rabinovich–Fabrikant model

Zulqurnain Sabir [a,b], Dumitru Baleanu [c,d,e,f], Sharifah E Alhazmi [g], Salem Ben Said [h,*]

[a] Department of Mathematics and Statistics, Hazara University, Mansehra, Pakistan
[b] Department of Computer Science and Mathematics, Lebanese American University, Beirut, Lebanon
[c] Department of Mathematics, Cankaya University, Ankara, Turkey
[d] Institute of Space Sciences, Magurele, Romania
[e] Department of Medical Research, China Medical University Hospital, China Medical University, Taichung, Taiwan
[f] Near East University, Mathematics research center, Nicosia, 99138, North Cyprus, Mersin 10 Turkey
[g] Mathematics Department, Al-Qunfudah University College, Umm Al-Qura University, Mecca, USA
[h] Department of Mathematical Sciences, UAE University, P. O. Box 15551, Al Ain, United Arab Emirates

ARTICLE INFO

Keywords:
Rabinovich-Fabrikant
Genetic algorithm
Artificial neural networks
Active set method
Numerical solutions

ABSTRACT

The current study shows a reliable stochastic computing heuristic approach for solving the nonlinear Rabinovich-Fabrikant model. This nonlinear model contains three ordinary differential equations. The process of stochastic computing artificial neural networks (ANNs) has been applied along with the competences of global heuristic genetic algorithm (GA) and local search active set (AS) methodologies, i.e., ANNs-GAAS. The construction of merit function is performed through the differential Rabinovich-Fabrikant model. The results obtained through this scheme are simple, reliable, and accurate, which have been calculated to optimize the merit function by using the GAAS method. The comparison of the obtained results through this scheme and the conventional reference solutions strengthens the correctness of the proposed method. Ten numbers of neurons along with the log-sigmoid transfer function in the neural network structure have been used to solve the model. The values of the absolute error are performed around 10^{-07} and 10^{-08} for each class of the Rabinovich-Fabrikant model. Moreover, the reliability of the ANNs-GAAS approach is observed by using different statistical approaches for solving the Rabinovich-Fabrikant model.

1. Introduction

The famous researchers Rabinovich and Fabrikant introduced one of the significant Rabinovich-Fabrikant model that is based on the chaotic system. Firstly, the design of this model is used for the physical system, which describe stochasticity occurring through the modulation variability based on the dissipative non-equilibrium medium [1]. In recent years, the physical properties proved the exceptionally high dynamics of the model [2]. Most of the chaotic models involve nonlinearities based on the second order, like Lorenz system. However, the nonlinear third order Rabinovich-Fabrikant model is one of them that shows an extraordinary dynamic, e.g., "virtual" saddles alongside various chaotic attractive features with distinct forms and hidden chaotic attractions [3–10].

* Corresponding author.
E-mail addresses: zulqurnain.sabir@lau.edu.lb (Z. Sabir), dumitru@cankaya.edu.tr (D. Baleanu), sehazmi@uqu.edu.sa (S. E Alhazmi), salem.bensaid@uaeu.ac.ae (S. Ben Said).

https://doi.org/10.1016/j.heliyon.2023.e22030
Received 9 May 2023; Received in revised form 22 October 2023; Accepted 2 November 2023
Available online 7 November 2023

A significant competition for innovative researchers is provided by the mathematical modeling of nonlinear systems. This nonlinear system presents a realism chaotic model, which contains an ordinary differential form of three coupled equations based on the Anatoly Fabrikant and Mikhail Rabinovich using the pioneer investigations of Rabinovich and Fabrikant (1979). The mathematical representation of the model is represented by Eq. (1), shown as [11,12]:

$$\begin{cases} x'(u) = \left(x^2(u) + z(u) - 1\right)y(u) + cx(u), x(0) = m_1, \\ y'(u) = \left(-x^2(u) + 3z(u) + 1\right)x(u) + cy(u), y(0) = m_2, \\ z'(u) = -2(x(u)y(u) + d)z(u), z(0) = m_3. \end{cases} \tag{1}$$

In the above system, prime shows the derivative, m_1, m_1 and m_3 represent the inititial conditions, u is taken as input, while c and d are the finite real constant that are used to control the model's evolution. The above model has a great significance in various branches of physics and mathematics.

The aim of this research is to provide the stochastic computing artificial neural networks (ANNs) together with the capabilities of global and local search heuristics based genetic algorithm (GA) and active set (AS) schemes, i.e., ANNs-GAAS for presenting the solutions of the Rabinovich–Fabrikant model. The stochastic schemes-based numerical simulations are offered to present the solutions of the nonlinear natured models, e.g., singular systems of higher order singular [13,14], dengue fever dynamical model [15], fractional kind of the singular models [16,17], Lotka-Volterra model [18], functional differential models [19,20], SITR model [21,22], and heterogeneous environment mosquito dispersal model [23]. In the light of these representations, the authors are motivated to design the ANNs-GAAS scheme to solve the Rabinovich–Fabrikant model. For the solutions of the nonlinear model statistically, we apply typically few of the schemes, e.g., estimation of maximum likelihood or nonlinear regression. These schemes imply fitting a system to detect the data and estimate the parameters, which describe the variable relationship in the modelling. Some of the statistical data that can be suitable to solve a nonlinear system are data collection, model specification and data estimation. The novel inspirations of this study are reported as.

- The solution the Rabinovich–Fabrikant model is proposed effectively by using the designed computational ANNs-GAAS scheme.
- The trustworthy, consistent, and stable performances of the model validate the accurateness of the ANN-GAAS solver.
- The values of the absolute error (AE) perform in good practices that substantiate the trustworthiness of the computational ANNs-GAAS scheme.
- Based on a statistical analysis the computational method is validated in order to present the solutions of the model by using forty trials through the heuristic stochastic performances.

The remaining sections of the paper are presented as: Sect 2 shows the computational performances of the ANNs-GAAS scheme along with statistical measures. Sect 3 represents the solution impressions. Sect 4 is designed based on the concluding remarks.

2. Designed ANNs-GAAS scheme

The neural network nature has been presented in different studies, e.g., Clifford-valued neural networks with impulsive and time-varying delays effects [24], RBF neural network-based fault-tolerant active control [25], and delayed Clifford-valued recurrent neural networks [26]. The computational performances of the ANNs-GAAS approach are illustrated to solve numerically the given Rabinovich-Fabrikant model. A merit function based on the hybridization of GAAS scheme is also provided in this section.

2.1. Designed scheme

The neural network procedure is presented in Eq. (2) as:

$$\begin{aligned} [\hat{x}(u), \hat{y}(u), \hat{z}(u)] &= \left[\sum_{i=1}^{q} l_{x,i} R\left(w_{x,i}u + s_{x,i}\right), \sum_{i=1}^{q} l_{y,i} R\left(w_{y,i}u + s_{y,i}\right), \sum_{i=1}^{q} l_{z,i} R\left(w_{z,i}u + s_{z,i}\right)\right], \\ [\hat{x}'(u), \hat{y}'(u), \hat{z}'(u)] &= \left[\sum_{i=1}^{q} l_{x,i} R'\left(w_{x,i}u + s_{x,i}\right), \sum_{i=1}^{q} l_{y,i} R'\left(w_{y,i}u + s_{y,i}\right), \sum_{i=1}^{q} l_{z,i} R'\left(w_{z,i}u + s_{z,i}\right)\right], \end{aligned} \tag{2}$$

where, R is the transfer function, q shows the number of neurons, the hat terms represent the proposed solutions, and W is an unidentified weight vector, given as: $\boldsymbol{W} = [\boldsymbol{W_x}, \boldsymbol{W_y}, \boldsymbol{W_z}]$, for $\boldsymbol{W_x} = [\boldsymbol{l_x}, \boldsymbol{\omega_x}, \boldsymbol{s_x}]$, $\boldsymbol{W_y} = [\boldsymbol{l_y}, \boldsymbol{\omega_y}, \boldsymbol{s_y}]$, and $\boldsymbol{W_z} = [\boldsymbol{l_z}, \boldsymbol{\omega_z}, \boldsymbol{s_z}]$, where

$$\begin{aligned} l_x &= \left[l_{x,1}, l_{x,2}, \ldots, l_{x,q}\right], w_x = \left[w_{x,1}, w_{x,2}, \ldots, w_{x,q}\right], s_x = \left[s_{x,1}, s_{x,2}, \ldots, s_{x,q}\right], \\ l_y &= \left[l_{y,1}, l_{y,2}, \ldots, l_{y,q}\right], w_y = \left[w_{y,1}, w_{y,2}, \ldots, w_{y,q}\right], s_y = \left[s_{y,1}, s_{y,2}, \ldots, s_{y,q}\right], \\ l_z &= \left[l_{z,1}, l_{z,2}, \ldots, l_{z,q}\right], w_z = \left[w_{z,1}, w_{z,2}, \ldots, w_{z,q}\right], s_z = \left[s_{z,1}, s_{z,2}, \ldots, s_{z,q}\right]. \end{aligned}$$

The log-sigmoid activation function is $R(u) = \frac{1}{(1+\exp(-u))}$.

$$
\begin{aligned}
[\widehat{x}, \widehat{y}, \widehat{z}] &= \left[\sum_{i=1}^{q} \frac{l_{x,i}}{1+e^{-\left(w_{x,i}u+s_{x,i}\right)}}, \sum_{i=1}^{q} \frac{l_{y,i}}{1+e^{-\left(w_{y,i}u+s_{y,i}\right)}}, \sum_{i=1}^{q} \frac{l_{z,i}}{1+e^{-\left(w_{z,i}u+s_{z,i}\right)}}\right], \\
[\widehat{x}^{'}, \widehat{y}^{'}, \widehat{z}^{'}] &= \left[\sum_{i=1}^{q} \frac{l_{x,i}w_{x,i}e^{-\left(w_{x,i}u+s_{x,i}\right)}}{\left(1+e^{-\left(w_{x,i}u+s_{x,i}\right)}\right)^2}, \sum_{i=1}^{q} \frac{l_{y,i}w_{y,i}e^{-\left(w_{y,i}u+s_{y,i}\right)}}{\left(1+e^{-\left(w_{y,i}u+s_{y,i}\right)}\right)^2}, \sum_{i=1}^{q} \frac{l_{z,i}w_{z,i}e^{-\left(w_{z,i}u+s_{z,i}\right)}}{\left(1+e^{-\left(w_{z,i}u+s_{z,i}\right)}\right)^2}\right].
\end{aligned} \tag{3}
$$

The objective function is shown in Eqs. (1)–(8) as follows:

$$\Xi = \sum_{k=1}^{4} \Xi_k \tag{4}$$

$$\Xi_1 = \frac{1}{N}\sum_{p=1}^{N}\left[\widehat{x}_p^{'} - \left(\widehat{z}_p + x_p^2 - 1\right)\widehat{y}_p - c\widehat{x}_p\right]^2, \tag{5}$$

$$\Xi_2 = \frac{1}{N}\sum_{p=1}^{N}\left[\widehat{y}_p^{'} - \left(1 - x_p^2 + 3\widehat{z}_p\right)\widehat{x}_p - c\widehat{y}_p\right]^2, \tag{6}$$

$$\Xi_3 = \frac{1}{N}\sum_{p=1}^{N}\left[\widehat{z}_p^{'} + 2\left(d + \widehat{x}_p\widehat{y}_p\right)\widehat{z}_p\right]^2, \tag{7}$$

$$\Xi_4 = \frac{1}{3}\left[(\widehat{x}_0 - m_1)^2 + (\widehat{y}_0 - m_2)^2 + (\widehat{z}_0 - m_3)^2\right], \tag{8}$$

where $\widehat{x}_p = x(u_p), \widehat{y}_p = y(u_p), \widehat{z}_p = z(u_p), Nh = 1,$ and $u_p = hp$.

2.2. Optimization: ANNs-GAAS procedure

There are various optimization procedures that have been used in the literature, some of them are evolutionary many-objective algorithm [27], adaptive polyploid memetic algorithm [28], universal island-based metaheuristic approach [29], a novel memetic algorithm [30], NSGA-II and MOPSO algorithms [31]. In this study, the optimization performances based on the ANNs-GAAS have been presented for the solution of the Rabinovich-Fabrikant model.

GA is a popular global search technique based on the optimization, which has been used to present the solutions of both nonlinear and linear networks. Additionally, it is conducted by utilizing the feature selection processes in order to manage both types of the models, constrained and unconstrained. Typically, GA works to standardize the outcomes of a specific population for resolving difficult approaches based on the optimal training. Recently, it is executed in various applications, some of them are categorize the biomarker genes [32], diabetes prediction [33], digital twin robots [34], feature diversity in cancer microarray [35], evaluate soil liquefaction potential [36], system of vehicle routing [37], prediction of adsorption capacity of nanocomposite materials [38], optimization of cloud service model [39], and liver disease model [40].

Table 1
Pseudocode for the Rabinovich–Fabrikant model.

GA process start

Inputs: For the same networks of the elements, the chromosomes are presented as: $\boldsymbol{W} = [\boldsymbol{l}, \boldsymbol{w}, \boldsymbol{s}]$
Population: Chromosomes vectors are $\boldsymbol{W}_x = [\boldsymbol{l}_x, \boldsymbol{\omega}_x, \boldsymbol{s}_x]$, $\boldsymbol{W}_y = [\boldsymbol{l}_y, \boldsymbol{\omega}_y, \boldsymbol{s}_y]$, and $\boldsymbol{W}_z = [\boldsymbol{l}_z, \boldsymbol{\omega}_z, \boldsymbol{s}_z]$.
Output: Best global weight vectors are $\boldsymbol{W}_{\mathbf{GA}}$
Start: The chromosomes selection is adjusted as $\boldsymbol{W}_{\mathbf{GA}}$.
Fitness Valuation: Adapt the Fitness (Ξ) for Eqs 4-8.

- **Stopping standards:** Conclude if [Ξ = TolCon = 10^{-20}], [Iterations = 70], [TolFun = 10^{-21}], [PopSize = 270] and [StallLimit = 120].

Go to **[storage]**
Ranking: Best $\boldsymbol{W}_{\mathbf{GA}}$ performances.
Storage: $\boldsymbol{W}_{\mathbf{GA}}$, time, generation, function count, Ξ for GA values
GA process ends
AS procedure Starts
Inputs: W_{GA}
Output: Optimal GAASA weights are presented as $\boldsymbol{W}_{\mathbf{GAAS}}$
Initialize: Assignments, $\boldsymbol{W}_{\mathbf{GAAS}}$ best values, & generations.
Termination standards: Terminate if [MaxFunEvals = 250000], [TolX = Ξ = TolFun = 10^{-21}], & [Iterations = 500].
FIT computation: $\boldsymbol{W}_{\mathbf{GAAS}}$ and Ξ based Eqs 4–8.
Adjustments: Standardize 'fmincon' using AS approach, Ξ to improve '**W**'.
Accumulate: Transubstantiate iterations $\boldsymbol{W}_{\mathbf{GAAS}}$, Ξ, time, & func counts for AS trials.
AS scheme End

Active set approach is an optimization local search procedures to investigate both models using the unconstrained/constrained systems. It provides an effective approach to calculate the results accurately. Recently, AS method is applied in various submissions, embedded model predictive control [41], derivative-free nonlinear bound-constrained optimization [42], intensity inhomogeneities [43], fast model predictive control and min-max robust control [44,45]. The procedure-based GAAS approach is directed to lower the slowness of the global scheme. The pseudocode using the GAAS approach is shown in Table 1.

2.3. Performance indices

The statistical semi-interquartile range (SIR), Theil's inequality coefficient (TIC) and variance account for (VAF) measures are presented in Eqs. 9–11 as:

$$\begin{cases} \mathrm{SIR} = -\dfrac{1}{2}(Q_1 - Q_3), \\ Q_1 = 1^{\mathrm{st}}\mathrm{quartile}, Q_3 = 3^{\mathrm{rd}}\mathrm{quartile}, \end{cases} \tag{9}$$

$$\begin{cases} \left[\mathrm{VAF}_x, \mathrm{VAF}_y, \mathrm{VAF}_z\right] = \begin{bmatrix} \left(1 - \dfrac{\mathrm{var}\left(x_p - \widehat{x}_p\right)}{\mathrm{var}\left(x_p\right)}\right)*100, \left(1 - \dfrac{\mathrm{var}\left(y_p - \widehat{y}_p\right)}{\mathrm{var}\left(y_p\right)}\right)*100, \\ \left(1 - \dfrac{\mathrm{var}\left(z_p - \widehat{z}_p\right)}{\mathrm{var}\left(z_p\right)}\right)*100, \end{bmatrix}, \\ \left[\mathrm{EVAF}_x, \mathrm{EVAF}_y, \mathrm{EVAF}_z\right] = \left[\left|100 - \mathrm{VAF}_x\right|, \left|100 - \mathrm{VAF}_y\right|, \left|100 - \mathrm{VAF}_z\right|\right], \end{cases} \tag{10}$$

$$\left[\mathrm{TIC}_x, \mathrm{TIC}_y, \mathrm{TIC}_z\right] = \begin{bmatrix} \dfrac{\sqrt{\dfrac{1}{n}\sum\limits_{p=1}^{n}\left(x_p - \widehat{x}_p\right)^2}}{\left(\sqrt{\dfrac{1}{n}\sum\limits_{p=1}^{n}x_p^2} + \sqrt{\dfrac{1}{n}\sum\limits_{p=1}^{n}\widehat{x}_p^2}\right)}, \dfrac{\sqrt{\dfrac{1}{n}\sum\limits_{p=1}^{n}\left(y_p - \widehat{y}_p\right)^2}}{\left(\sqrt{\dfrac{1}{n}\sum\limits_{p=1}^{n}y_p^2} + \sqrt{\dfrac{1}{n}\sum\limits_{p=1}^{n}\widehat{y}_p^2}\right)}, \\ \dfrac{\sqrt{\dfrac{1}{n}\sum\limits_{p=1}^{n}\left(z_p - \widehat{z}_p\right)^2}}{\left(\sqrt{\dfrac{1}{n}\sum\limits_{p=1}^{n}z_p^2} + \sqrt{\dfrac{1}{n}\sum\limits_{p=1}^{n}\widehat{z}_p^2}\right)} \end{bmatrix}. \tag{11}$$

In the above network EVAF shows the error in VAF.

3. Numerical results and discussions

The numerical solutions of the Rabinovich–Fabrikant model are obtained through the stochastic performances based on the ANNs-GAAS approach and presented in this part. The results overlapping, weight vectors, performance measures, and AE plots have also been provided. The mathematical formulations of the model are shown in Eq. (12) as:

$$\begin{cases} x'(u) = \left(x^2(u) + z(u) - 1\right)y(u) + 2x(u), x(0) = 0.1, \\ y'(u) = \left(-x^2(u) + 3z(u) + 1\right)x(u) + 2y(u), y(0) = 0.2, \\ z'(u) = -2(x(u)y(u) + 3)z(u), z(0) = 0.3. \end{cases} \tag{12}$$

An objective function based on Eq (4) is presented in Eq (13) as:

$$\Xi = \frac{1}{N}\sum_{K=1}^{N}\begin{pmatrix} \left[\left[\widehat{x}'_p - \left(\widehat{x}_p^2 + \widehat{z}_p - 1\right)\widehat{y}_p - 2\widehat{x}_p\right]\right]^2 \\ + \left[\widehat{y}'_p - \left(-\widehat{x}_p^2 + 3\widehat{z}_p + 1\right)\widehat{x}_p - 2\widehat{y}_p\right]^2 \\ + \left[\widehat{z}'_p + 2\left(3 + \widehat{x}_p\widehat{y}_p\right)\widehat{z}_p\right]^2 \end{pmatrix} + \frac{1}{3}\left[(\widehat{x}_0 - 0.1)^2 + (\widehat{y}_0 - 0.2)^2 + (\widehat{z}_0 - 0.3)^2\right]. \tag{13}$$

The optimization is performed in system (1) using the ANNs-GAAS approach for illustrating numerically the dynamics of the nonlinear Rabinovich–Fabrikant model. The parameters of the neural network parameters have been achieved for ten numbers of neurons. The values of the best weights have been achieved and used in the first part of Eq (3). These best weights values are derived to solve the Rabinovich–Fabrikant model, which are given in Eqs. 14–16 as:

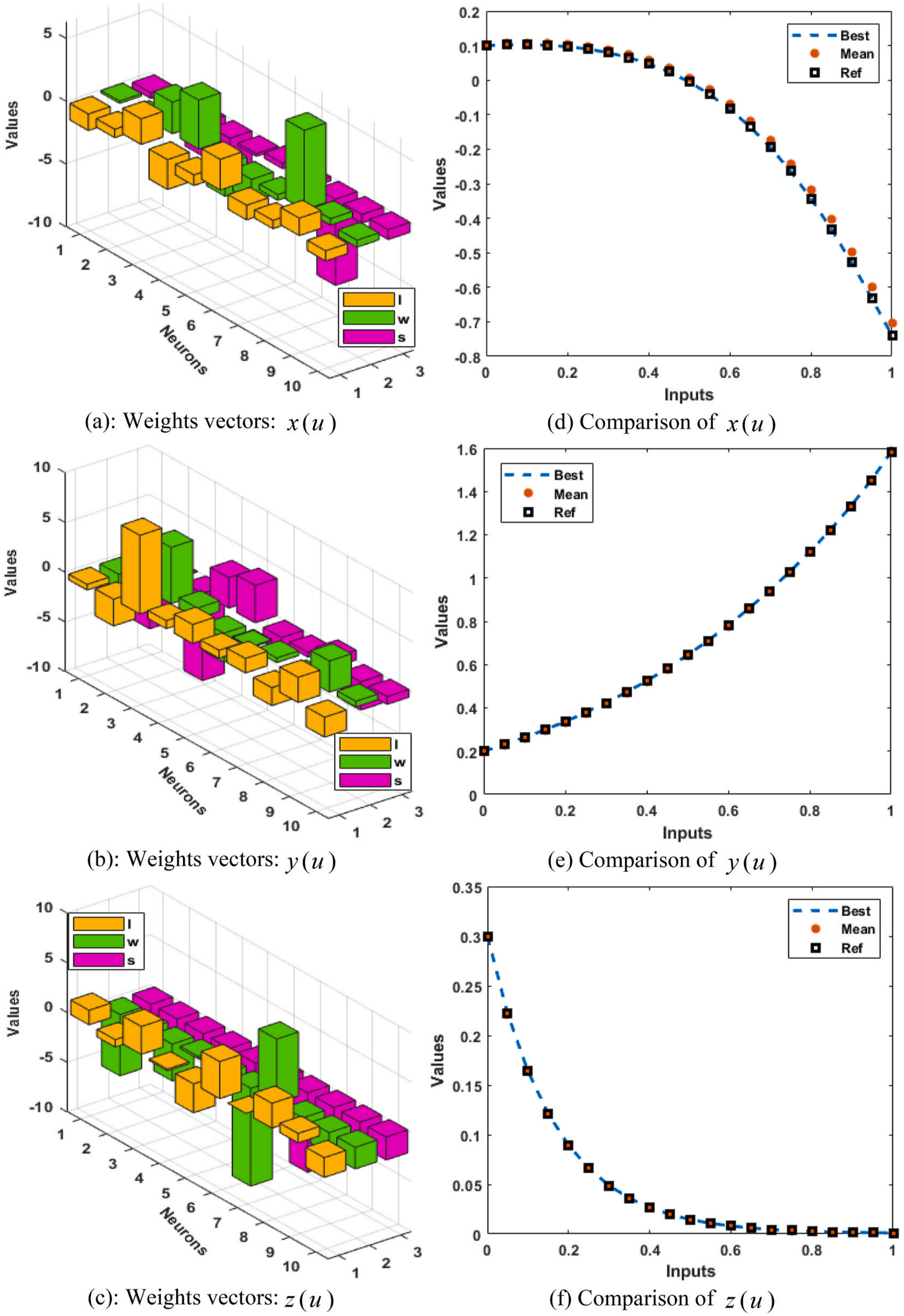

Fig. 1. Weight vectors and results to solve the Rabinovich–Fabrikant model.

$$
\begin{aligned}
\widehat{x}(u)= & \frac{-1.3190}{1+e^{-(0.1867u-04501)}}-\frac{0.6729}{1+e^{-(-0.6919u-0.2921)}}+\frac{2.0336}{1+e^{-(2.5193u-2.6580)}}-\frac{2.3759}{1+e^{-(3.8864u-3.7874)}}-\frac{0.8546}{1+e^{-(-2.5543u-0.221)}} \\
& +\frac{2.4417}{1+e^{-(-1.7558u+0.4287)}}-\frac{1.1682}{1+e^{-(0.4529u-0.331)}}-\frac{0.6590}{1+e^{-(6.3242u-6.8694)}} \\
& +\frac{1.3934}{1+e^{-(0.5065u-0.6938)}}-\frac{0.8111}{1+e^{-(-0.5551u-0.7911)}},
\end{aligned} \tag{14}
$$

$$
\begin{aligned}
\widehat{y}(u)= & \frac{-0.5665}{1+e^{-(-2.5912u-6.5235)}}-\frac{2.6929}{1+e^{-(-0.223u-0.0234)}}+\frac{7.9010}{1+e^{-(5.6499u-8.7701)}}+\frac{0.8084}{1+e^{-(1.0445u+3.0604)}} \\
& +\frac{1.9053}{1+e^{-(-2.9376u+3.7511)}}+\frac{0.7949}{1+e^{-(0.1006u-1.4452)}}+\frac{1.4496}{1+e^{-(00.4672u-0.4889)}}-\frac{1.8005}{1+e^{-(-0.502u+0.990)}} \\
& +\frac{2.5282}{1+e^{-(3.1352u-2.8383)}}-\frac{2.0067}{1+e^{-(0.5701u-0.7818)}},
\end{aligned} \tag{15}
$$

$$
\begin{aligned}
\widehat{z}(u)= & \frac{1.4672}{1+e^{-(-6.158u-1.9789)}}-\frac{0.7453}{1+e^{-(-2.009u-1.7919)}}+\frac{2.8028}{1+e^{-(-3.7065u-2.7569)}}-\frac{0.1683}{1+e^{-(0.2319u-3.4650)}}-\frac{2.9041}{1+e^{-(1.8675u-2.6734)}} \\
& +\frac{3.7189}{1+e^{-(9.8288u-4.2004)}}+\frac{0.0029}{1+e^{-(6.4296u-7.9947)}}+\frac{2.4959}{1+e^{-(-1.7097u-1.9491)}} \\
& +\frac{0.9486}{1+e^{-(-2.114u-2.5806)}}-\frac{1.9933}{1+e^{-(-2.1711u-2.3145)}}.
\end{aligned} \tag{16}
$$

The optimal weights of the Rabinovich–Fabrikant model and the comparison of obtained results for each dynamic of the model are represented in Fig. 1. These weights are obtained in Fig. 1 (a to c) through the stochastic ANNs-GAAS approach by using ten neurons that have been observed in Eqs 14–16. The overlapping of the best, and mean solutions is performed in Fig. 1(d–f), which shows the correctness of the ANNs-GAAS scheme for solving the Rabinovich–Fabrikant model. Fig. 2 presents the best/mean AE for the

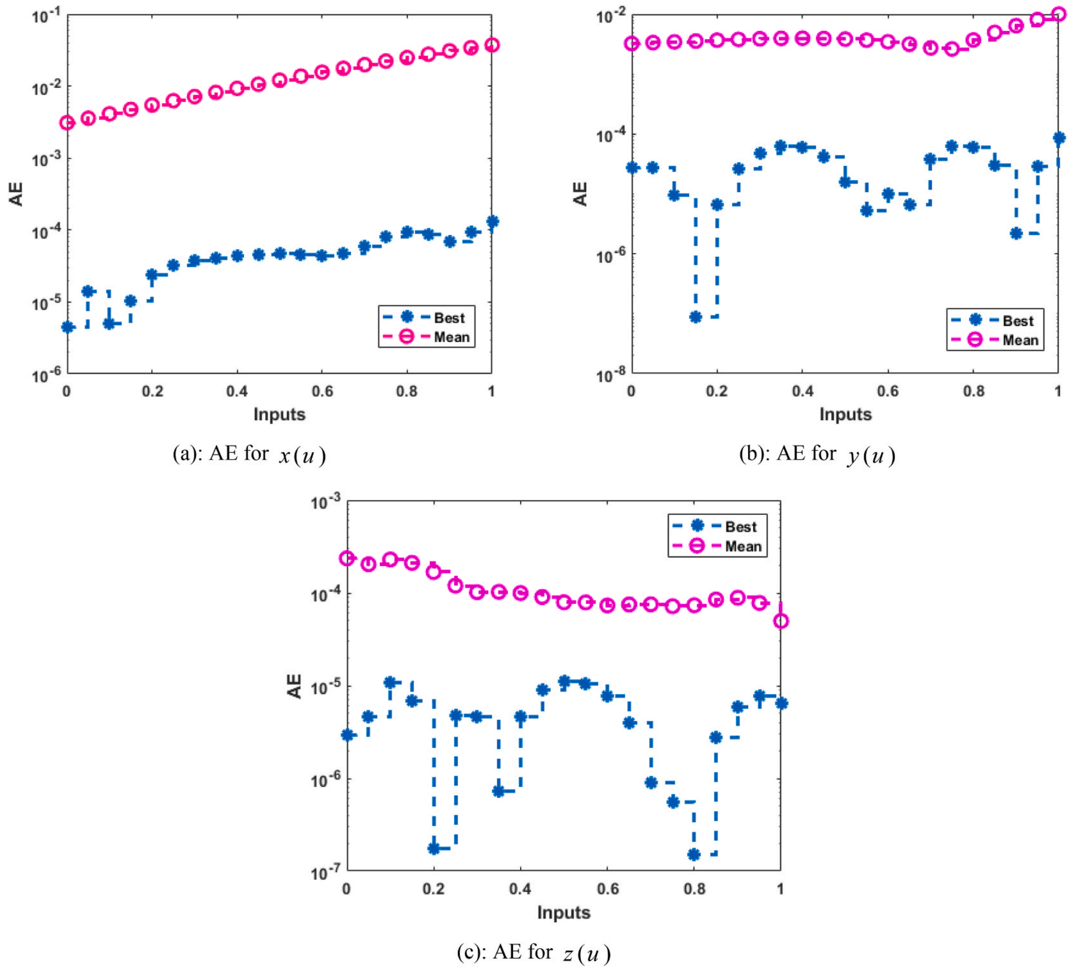

(a): AE for $x(u)$

(b): AE for $y(u)$

(c): AE for $z(u)$

Fig. 2. AE performances for the Rabinovich–Fabrikant model.

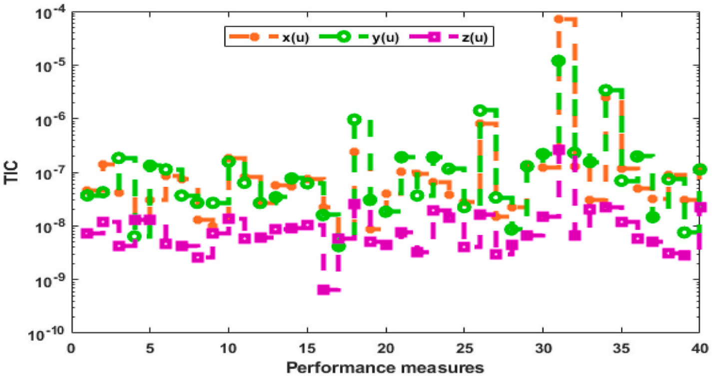

TIC operator values for the Rabinovich–Fabrikant model

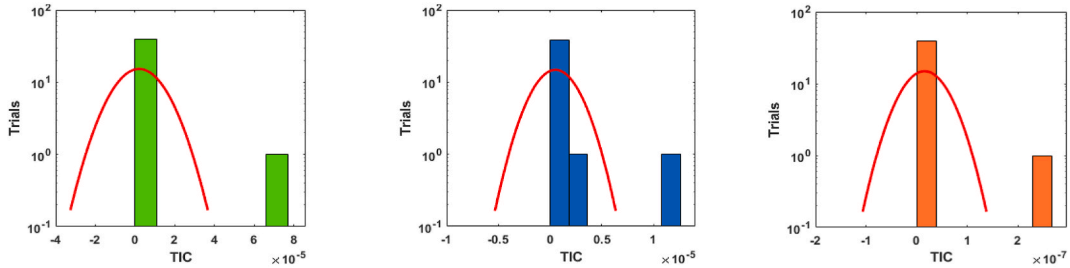

(a) Histograms $x(u)$ (b) Histograms $y(u)$ (c) Histograms $z(u)$

Fig. 3. TIC operator performances and histogram for the Rabinovich–Fabrikant model.

Rabinovich–Fabrikant model. It is presented that the optimal values are found as 10^{-05}-10^{-06}, 10^{-04}-10^{-07} and 10^{-05}-10^{-07}, whereas the mean AE values are calculated around 10^{-02}-10^{-03}, 10^{-02}-10^{-04} and 10^{-03}-10^{-04} for each dynamic of the model shown in Fig. 2 (a to c) respectively. These negligible AE measures enhance the accuracy of the proposed ANNs-GAAS approach for solving the Rabinovich-Fabrikant model. The performances of TIC operator for the Rabinovich–Fabrikant model is shown in Fig. 3. These values are performed as 10^{-06} to 10^{-09} for each dynamic of the model as shown in Fig. 3 (a to c) respectively. The EVAF performances for solving the Rabinovich–Fabrikant model by using the ANNs-GAAS approach is presented in Fig. 4. These measures are reported as 10^{-05} to 10^{-08} for each class of the model shown in Fig. 4 (a to c) respectively. These best statistical operator representations obtained by the ANNs-GAAS solver enhance the reliability of the scheme for the Rabinovich–Fabrikant model.

Tables 2–4 presents the statistical performances based on the operator's minimum (best solutions), mean, maximum (worst solutions), standard deviation (SD), SIR and median. The minimum operator values are performed 10^{-05}-10^{-06} for first two categories of the model, while 10^{-06}-10^{-08} is performed for the 3rd class. The maximum values have been achieved on the behalf of worst solutions that are performed as 10^{-01}-10^{-02} for $x(u)$ and $y(u)$, while these values are calculated as 10^{-03}-10^{-04} for $z(u)$. The values of mean, SIR and median are performed around 10^{-04}-10^{-05} for each class of the Rabinovich–Fabrikant model. Likewise, the SD is reported as 10^{-02}-10^{-03} for $x(u)$ and $y(u)$, while the class $z(u)$ is performed as 10^{-04}-10^{-05}. On the behalf of these statistical representations, it is approved that the ANNs-GAAS solver performs accurate for solving the Rabinovich–Fabrikant model.

4. Concluding remarks

In this study, a reliable stochastic computing heuristic scheme is presented to solve the nonlinear Rabinovich-Fabrikant model. This nonlinear model contains the systems of ordinary differential equations. Few concluding remarks of this research are presented as.

- The stochastic computing procedures along with the competences of both the local and global heuristic search techniques have been presented successfully to get the numerical results of the model.
- By utilizing the differential form of the Rabinovich-Fabrikant model, an objective function has been generated.
- The results obtained from this scheme are simple, reliable, and accurate, which have been calculated to optimize the merit function by using the GAAS method.
- The comparison of the obtained results through the proposed stochastic solver and the conventional reference solutions develops the precision of the proposed method.
- Ten numbers of neurons along with the log-sigmoid transfer function in the neural network structure have been presented to solve the model.
- The AE values have been performed in negligible measures, i.e., 10^{-04} to 10^{-07} to solve the model.

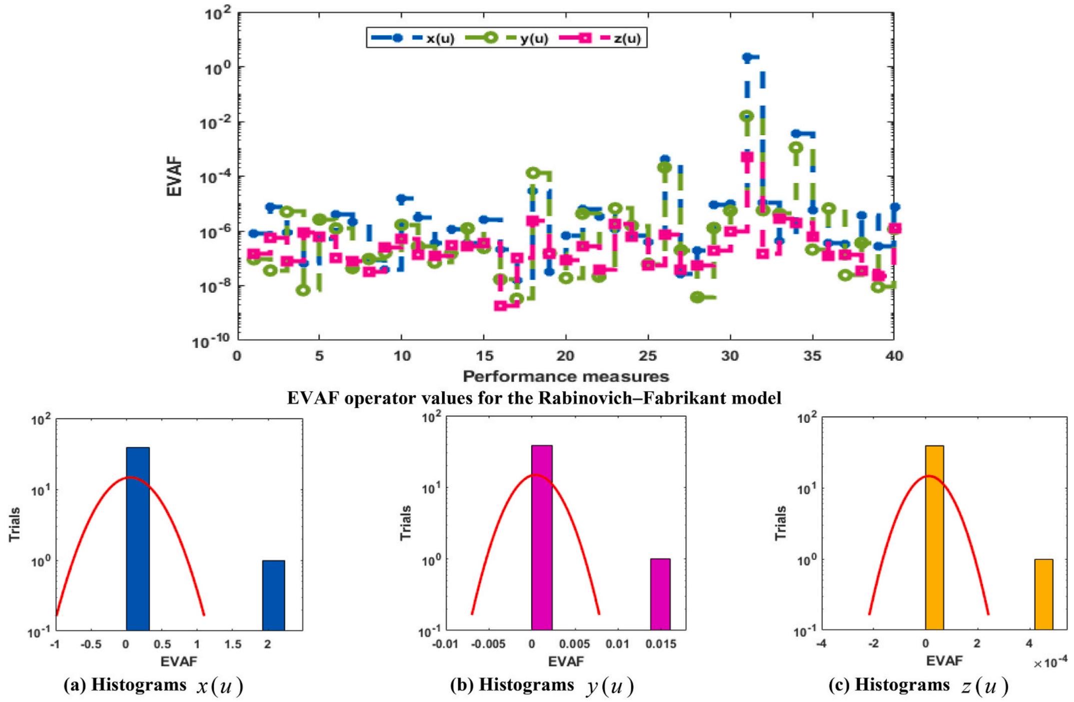

Fig. 4. EVAF operator performances and histogram for the Rabinovich–Fabrikant model.

Table 2
Statistical performances of the Rabinovich–Fabrikant model based dynamic (1).

u	$x(u)$					
	Minimum	**Maximum**	**Median**	**Mean**	**SIR**	**SD**
0	2.29807E-06	1.17960E-01	7.78760E-05	3.09055E-03	5.80774E-05	1.86299E-02
0.05	5.34403E-06	1.36422E-01	9.45818E-05	3.56899E-03	7.49867E-05	2.15460E-02
0.1	5.02689E-06	1.57107E-01	1.19284E-04	4.11966E-03	9.77564E-05	2.48109E-02
0.15	8.76056E-06	1.80476E-01	1.22573E-04	4.74257E-03	1.25893E-04	2.85003E-02
0.2	2.88105E-06	2.06929E-01	1.70157E-04	5.45233E-03	1.46296E-04	3.26763E-02
0.25	2.25170E-05	2.36837E-01	2.44879E-04	6.25464E-03	1.68468E-04	3.73974E-02
0.3	1.75530E-06	2.70570E-01	2.45932E-04	7.14778E-03	1.77008E-04	4.27244E-02
0.35	3.84417E-05	3.08521E-01	2.32414E-04	8.15354E-03	1.88363E-04	4.87181E-02
0.4	2.80217E-05	3.51123E-01	2.09657E-04	9.29374E-03	1.84915E-04	5.54457E-02
0.45	3.81863E-05	3.98855E-01	3.13247E-04	1.05966E-02	1.82256E-04	6.29815E-02
0.5	2.06341E-05	4.52249E-01	4.13603E-04	1.20665E-02	2.26978E-04	7.14115E-02
0.55	3.64150E-05	5.11884E-01	4.40580E-04	1.37304E-02	3.19349E-04	8.08241E-02
0.6	1.07381E-05	5.78365E-01	4.56319E-04	1.55965E-02	4.09627E-04	9.13142E-02
0.65	1.58786E-06	6.52284E-01	4.54974E-04	1.76331E-02	4.55046E-04	1.02982E-01
0.7	3.08380E-05	7.34164E-01	5.38844E-04	1.98414E-02	4.94618E-04	1.15912E-01
0.75	1.54075E-06	8.24366E-01	6.17158E-04	2.22387E-02	5.47668E-04	1.30161E-01
0.8	1.43090E-05	9.22975E-01	7.16249E-04	2.48563E-02	5.75919E-04	1.45739E-01
0.85	3.58919E-05	1.02965E-01	7.54127E-04	2.77171E-02	6.54851E-04	1.62589E-01
0.9	8.07321E-06	1.14349E-01	7.07870E-04	3.08240E-02	7.37787E-04	1.80561E-01
0.95	6.14115E-06	1.26282E-01	7.78635E-04	3.40968E-02	8.35359E-04	1.99393E-01
1	2.24218E-05	1.38515E-01	8.61990E-04	3.72679E-02	8.84715E-04	2.18711E-01

- For the Rabinovich-Fabrikant system, reliability of the ANNs-GAAS approach has been validated through several different statistical performances.

Future research direction

the ANN-GAAS solver is accomplished to perform the highly nonlinear singular systems [46,47], biological differential models [48, 49], nonlinear dynamics of the models [50–52], fractional differential model [53,54], cylindrical nonlinear Schrödinger equation [55], and pseudoplastic nanofluid flow [56].

Table 3
Statistical performances of the Rabinovich–Fabrikant model based dynamic (2).

u	$y(u)$					
	Minimum	**Maximum**	**Median**	**Mean**	**SIR**	**SD**
0	2.08982E-06	1.06554E-01	2.36713E-04	3.09055E-03	1.70428E-04	1.68356E-02
0.05	1.67399E-05	1.08687E-01	2.58620E-04	3.56899E-03	2.00865E-04	1.71802E-02
0.1	7.14048E-06	1.10210E-01	2.51623E-04	4.11966E-03	1.90543E-04	1.74335E-02
0.15	8.70039E-08	1.11128E-01	2.89002E-04	4.74257E-03	1.95656E-04	1.75925E-02
0.2	6.49360E-06	1.11394E-01	3.32881E-04	5.45233E-03	2.39311E-04	1.76528E-02
0.25	2.59795E-05	1.10909E-01	3.59807E-04	6.25464E-03	2.49967E-04	1.76022E-02
0.3	3.88400E-05	1.09508E-01	4.16517E-04	7.14778E-03	2.79696E-04	1.74181E-02
0.35	8.46055E-06	1.06961E-01	4.67783E-04	8.15354E-03	3.39667E-04	1.70662E-02
0.4	4.09436E-06	1.02963E-01	5.11579E-04	9.29374E-03	4.03179E-04	1.64998E-02
0.45	3.89728E-06	9.71268E-02	5.12757E-04	1.05966E-02	4.46287E-04	1.56659E-02
0.5	1.51777E-05	8.89783E-02	5.41587E-04	1.20665E-02	4.86843E-04	1.45033E-02
0.55	5.24651E-06	7.79517E-02	5.70686E-04	1.37304E-02	5.53658E-04	1.29533E-02
0.6	1.00694E-05	6.33936E-02	6.04871E-04	1.55965E-02	5.90022E-04	1.09856E-02
0.65	6.61441E-06	4.45779E-02	6.45056E-04	1.76331E-02	7.04403E-04	8.68834E-03
0.7	1.38398E-05	3.51697E-02	7.19404E-04	1.98414E-02	7.66781E-04	6.62055E-03
0.75	3.98738E-05	3.77281E-02	7.75046E-04	2.22387E-02	8.07751E-04	6.49767E-03
0.8	1.95105E-05	4.48265E-02	7.40852E-04	2.48563E-02	8.43831E-04	9.62262E-03
0.85	1.99012E-05	8.74965E-02	7.18474E-04	2.77171E-02	9.70622E-04	1.53443E-02
0.9	2.23719E-06	1.36737E-01	7.50571E-04	3.08240E-02	1.13654E-03	2.26467E-02
0.95	2.92128E-05	1.91750E-01	8.83480E-04	3.40968E-02	1.26668E-03	3.10850E-02
1	8.14854E-05	2.50903E-01	1.10698E-03	3.72679E-02	1.36637E-03	4.03115E-02

Table 4
Statistical performances of the Rabinovich–Fabrikant model based dynamic (3).

u	$z(u)$					
	Minimum	**Maximum**	**Median**	**Mean**	**SIR**	**SD**
0	2.57152E-06	6.82109E-03	3.42049E-05	3.09055E-03	3.15065E-05	1.07187E-03
0.05	1.79312E-06	5.19011E-03	5.76426E-05	3.56899E-03	3.53598E-05	8.11871E-04
0.1	4.85310E-06	4.17777E-03	9.78632E-05	4.11966E-03	8.55330E-05	6.49865E-04
0.15	2.14033E-06	3.44454E-03	8.79933E-05	4.74257E-03	1.08183E-04	5.39613E-04
0.2	1.73908E-07	2.85134E-03	5.68566E-05	5.45233E-03	7.20857E-05	4.48046E-04
0.25	2.27467E-06	2.34814E-03	2.80906E-05	6.25464E-03	4.04881E-05	3.69593E-04
0.3	2.69486E-06	1.91946E-03	4.85180E-05	7.14778E-03	2.44358E-05	2.99245E-04
0.35	7.31215E-07	1.56022E-03	5.81746E-05	8.15354E-03	2.63838E-05	2.40502E-04
0.4	2.94999E-06	1.26654E-03	5.60883E-05	9.29374E-03	3.22862E-05	1.95961E-04
0.45	8.63087E-08	1.03282E-03	4.83960E-05	1.05966E-02	3.93159E-05	1.63523E-04
0.5	3.10594E-06	8.51451E-04	3.97937E-05	1.20665E-02	2.91943E-05	1.38276E-04
0.55	1.79336E-06	7.14384E-04	5.41125E-05	1.37304E-02	2.51677E-05	1.13121E-04
0.6	4.36420E-07	6.13222E-04	5.10589E-05	1.55965E-02	3.42948E-05	1.00069E-04
0.65	1.73022E-06	5.40304E-04	5.64359E-05	1.76331E-02	2.83221E-05	8.88963E-05
0.7	7.66474E-07	4.89001E-04	5.36105E-05	1.98414E-02	3.35518E-05	8.45095E-05
0.75	5.50166E-07	4.53772E-04	3.97511E-05	2.22387E-02	4.24631E-05	8.82930E-05
0.8	1.52746E-07	4.30266E-04	3.42216E-05	2.48563E-02	3.67141E-05	9.20994E-05
0.85	2.71899E-06	4.15335E-04	5.09480E-05	2.77171E-02	3.31115E-05	8.86452E-05
0.9	5.89255E-06	4.06757E-04	6.87730E-05	3.08240E-02	3.39482E-05	8.42700E-05
0.95	3.56278E-06	4.03273E-04	5.60421E-05	3.40968E-02	3.23000E-05	7.73961E-05
1	1.36096E-06	4.04407E-04	2.35880E-05	3.72679E-02	1.43115E-05	7.90665E-05

Data availability

No data was used for the research described in the article.

Additional information

No additional information is available for this paper.

CRediT authorship contribution statement

Zulqurnain Sabir: Writing – review & editing, Writing – original draft, Project administration. **Dumitru Baleanu:** Writing – review & editing, Writing – original draft, Project administration. **Sharifah E Alhazmi:** Writing – review & editing, Writing – original draft, Project administration. **Salem Ben Said:** Writing – review & editing, Writing – original draft, Project administration.

Declaration of competing interest

All the authors of the manuscript declare that there are no potential conflicts of interest.

Acknowledgement

The author (sehazmi@uqu.edu.sa) convey their gratitude to the Deanship for Research & Innovation, Ministry of Education in Saudi Arabia for supporting this under the research project number: IFP22UQU4282396DSR052.

References

[1] M.I. Rabinovich, A.L. Fabrikant, Stochastic self-modulation of waves in nonequilibrium media, J. Exp. Theor. Phys. 77 (1979) 617–629.
[2] M.F. Danca, M. Feckan, N. Kuznetsov, G. Chen, Looking more closely at the Rabinovich–Fabrikant system, International Journal of Bifurcation and Chaos 26 (2) (2016), 1650038.
[3] Y. Liu, Q. Yang, G. Pang, A hyperchaotic system from the Rabinovich system, J. Comput. Appl. Math. 234 (1) (2010) 101–113.
[4] S.S. Motsa, P.G. Dlamini, M. Khumalo, Solving hyperchaotic systems using the spectral relaxation method, in: Abstract and Applied Analysis, vol. 2012, Hindawi, 2012, January.
[5] C.X. Zhang, S.M. Yu, Y. Zhang, Design and realization of multi-wing chaotic attractors via switching control, Int. J. Mod. Phys. B 25 (16) (2011) 2183–2194.
[6] I. Chairez, Multiple DNN identifier for uncertain nonlinear systems based on Takagi–Sugeno inference, Fuzzy Set Syst. 237 (2014) 118–135.
[7] S.K. Agrawal, M. Srivastava, S. Das, Synchronization between fractional-order Ravinovich–Fabrikant and Lotka–Volterra systems, Nonlinear Dynam. 69 (2012) 2277–2288.
[8] M.F. Danca, N. Kuznetsov, G. Chen, Unusual dynamics and hidden attractors of the Rabinovich–Fabrikant system, Nonlinear Dynam. 88 (2017) 791–805.
[9] M. Srivastava, S.K. Agrawal, K. Vishal, S. Das, Chaos control of fractional order Rabinovich–Fabrikant system and synchronization between chaotic and chaos controlled fractional order Rabinovich–Fabrikant system, Appl. Math. Model. 38 (13) (2014) 3361–3372.
[10] H. Serrano-Guerrero, C. Cruz-Hernández, R.M. López-Gutiérrez, L. Cardoza-Avendaño, R.A. ChávezPérez, Chaotic synchronization in nearest-neighbor coupled networks of 3D CNNs, J. Appl. Res. Technol. 11 (1) (2013) 26–41.
[11] K. Moaddy, A. Freihat, M. Al-Smadi, E. Abuteen, I. Hashim, Numerical investigation for handling fractional-order Rabinovich–Fabrikant model using the multistep approach, Soft Comput. 22 (3) (2018) 773–782.
[12] M.I. Rabinovich, A.L. Fabrikant, Stochastic self-modulation of waves in nonequilibrium media, J. Exp. Theor. Phys. 77 (1979) 617–629.
[13] Z. Sabir, S.A. Bhat, M.A.Z. Raja, S.E. Alhazmi, A swarming neural network computing approach to solve the Zika virus model, Eng. Appl. Artif. Intell. 126 (2023), 106924.
[14] Z. Sabir, M.A.Z. Raja, M.R. Ali, R. Sadat, I. Fathurrochman, R.A.S. Núñez, S.A. Bhat, A neuro Meyer wavelet neural network procedure for solving the nonlinear Leptospirosis model, Intelligent Systems with Applications (2023), 200243.
[15] M. Umar, Z. Sabir, M.A.Z. Raja, Y.G. Sánchez, A stochastic numerical computing heuristic of SIR nonlinear model based on dengue fever, Results Phys. 19 (2020), 103585.
[16] Z. Sabir, M.A.Z. Raja, M. Umar, M. Shoaib, Design of neuro-swarming-based heuristics to solve the third-order nonlinear multi-singular Emden–Fowler equation, The European Physical Journal Plus 135 (5) (2020) 410.
[17] Z. Sabir, M.A.Z. Raja, J.L. Guirao, T. Saeed, Meyer wavelet neural networks to solve a novel design of fractional order pantograph Lane-Emden differential model, Chaos, Solit. Fractals 152 (2021), 111404.
[18] M. Umar, Z. Sabir, M.A.Z. Raja, Intelligent computing for numerical treatment of nonlinear prey–predator models, Appl. Soft Comput. 80 (2019) 506–524.
[19] Z. Sabir, J.L. Guirao, T. Saeed, Solving a novel designed second order nonlinear Lane–Emden delay differential model using the heuristic techniques, Appl. Soft Comput. 102 (2021), 107105.
[20] J.L. Guirao, Z. Sabir, T. Saeed, Design and numerical solutions of a novel third-order nonlinear Emden–Fowler delay differential model, Math. Probl Eng. 2020 (2020).
[21] M. Umar, Z. Sabir, M.A.Z. Raja, F. Amin, T. Saeed, Y. Guerrero-Sanchez, Integrated neuro-swarm heuristic with interior-point for nonlinear SITR model for dynamics of novel COVID-19, Alex. Eng. J. 60 (3) (2021) 2811–2824.
[22] M. Umar, Z. Sabir, M.A.Z. Raja, M. Shoaib, M. Gupta, Y.G. Sánchez, A stochastic intelligent computing with neuro-evolution heuristics for nonlinear SITR system of novel COVID-19 dynamics, Symmetry 12 (10) (2020) 1628.
[23] M. Umar, M.A.Z. Raja, Z. Sabir, A.S. Alwabli, M. Shoaib, A stochastic computational intelligent solver for numerical treatment of mosquito dispersal model in a heterogeneous environment, The European Physical Journal Plus 135 (7) (2020) 1–23.
[24] G. Rajchakit, R. Sriraman, N. Boonsatit, P. Hammachukiattikul, C.P. Lim, P. Agarwal, Global exponential stability of Clifford-valued neural networks with time-varying delays and impulsive effects, Adv. Differ. Equ. 2021 (2021) 1–21.
[25] B. Wang, H. Jahanshahi, C. Volos, S. Bekiros, M.A. Khan, P. Agarwal, A.A. Aly, A new RBF neural network-based fault-tolerant active control for fractional time-delayed systems, Electronics 10 (12) (2021) 1501.
[26] N. Boonsatit, G. Rajchakit, R. Sriraman, C.P. Lim, P. Agarwal, Finite-/fixed-time synchronization of delayed Clifford-valued recurrent neural networks, Adv. Differ. Equ. 2021 (1) (2021) 1–25.
[27] Q. Gu, D. Pang, Q. Wang, Evolutionary Many-Objective Algorithm with Improved Growing Neural Gas and Angle-Penalized Distance for Irregular Problems, Applied Intelligence, 2023, pp. 1–30.
[28] M.A. Dulebenets, An Adaptive Polyploid Memetic Algorithm for Scheduling Trucks at a Cross-Docking Terminal, vol. 565, Information Sciences, 2021, pp. 390–421.
[29] M. Kavoosi, M.A. Dulebenets, O. Abioye, J. Pasha, O. Theophilus, H. Wang, R. Kampmann, M. Mikijeljević, Berth scheduling at marine container terminals: a universal island-based metaheuristic approach, Maritime Business Review 5 (1) (2019) 30–66.
[30] M.A. Dulebenets, A novel memetic algorithm with a deterministic parameter control for efficient berth scheduling at marine container terminals, Maritime Business Review 2 (4) (2017) 302–330.
[31] M. Rabbani, N. Oladzad-Abbasabady, N. Akbarian-Saravi, Ambulance routing in disaster response considering variable patient condition: NSGA-II and MOPSO algorithms, J. Ind. Manag. Optim. 18 (2) (2022) 1035–1062.
[32] M. Sathya, M. Jeyaselvi, S. Joshi, E. Pandey, P.K. Pareek, S.S. Jamal, V. Kumar, H.K. Atiglah, Cancer categorization using genetic algorithm to identify biomarker genes, Journal of Healthcare Engineering 2022 (2022).
[33] J. Abdollahi, B. Nouri-Moghaddam, Hybrid stacked ensemble combined with genetic algorithms for diabetes prediction, Iran Journal of Computer Science 5 (3) (2022) 205–220.
[34] X. Liu, D. Jiang, B. Tao, G. Jiang, Y. Sun, J. Kong, X. Tong, G. Zhao, B. Chen, Genetic algorithm-based trajectory optimization for digital twin robots, Front. Bioeng. Biotechnol. 9 (2022) 1433.
[35] S. Sayed, M. Nassef, A. Badr, I. Farag, A nested genetic algorithm for feature selection in high-dimensional cancer microarray datasets, Expert Syst. Appl. 121 (2019) 233–243.
[36] J. Zhou, S. Huang, T. Zhou, D.J. Armaghani, Y. Qiu, Employing a genetic algorithm and grey wolf optimizer for optimizing RF models to evaluate soil liquefaction potential, Artif. Intell. Rev. 55 (7) (2022) 5673–5705.

[37] Y. Wang, Y. Wei, X. Wang, Z. Wang, H. Wang, A clustering-based extended genetic algorithm for the multidepot vehicle routing problem with time windows and three-dimensional loading constraints, Appl. Soft Comput. 133 (2023), 109922.
[38] L.I. Weidong, M.K. Suhayb, L. Thangavelu, H.A. Marhoon, I. Pustokhina, U.F. Alqsair, A.S. El-Shafay, M. Alashwal, Implementation of AdaBoost and genetic algorithm machine learning models in prediction of adsorption capacity of nanocomposite materials, J. Mol. Liq. 350 (2022), 118527.
[39] Y. Yang, B. Yang, S. Wang, F. Liu, Y. Wang, X. Shu, A dynamic ant-colony genetic algorithm for cloud service composition optimization, Int. J. Adv. Des. Manuf. Technol. 102 (1–4) (2019) 355–368.
[40] M. Hassoon, M.S. Kouhi, M. Zomorodi-Moghadam, M. Abdar, Rule optimization of boosted c5. 0 classification using genetic algorithm for liver disease prediction, in: 2017 International Conference on Computer and Applications (Icca), IEEE, 2017, September, pp. 299–305.
[41] M. Klaučo, M. Kalúz, M. Kvasnica, Machine learning-based warm starting of active set methods in embedded model predictive control, Eng. Appl. Artif. Intell. 77 (2019) 1–8.
[42] S. Gratton, P.L. Toint, A. Tröltzsch, An active-set trust-region method for derivative-free nonlinear bound-constrained optimization, Optim. Methods Software 26 (4–5) (2011) 873–894.
[43] C. Li, R. Huang, Z. Ding, J.C. Gatenby, D.N. Metaxas, J.C. Gore, A level set method for image segmentation in the presence of intensity inhomogeneities with application to MRI, IEEE Trans. Image Process. 20 (7) (2011) 2007–2016.
[44] J. Buerger, M. Cannon, B. Kouvaritakis, An active set solver for min-max robust control, in: 2013 American Control Conference, IEEE, 2013, June, pp. 4221–4227.
[45] R. Quirynen, S. Di Cairano, PRESAS: Block-structured preconditioning of iterative solvers within a primal active-set method for fast model predictive control, Optim. Control Appl. Methods 41 (6) (2020) 2282–2307.
[46] Z. Sabir, M.R. Ali, I. Fathurrochman, M.A.Z. Raja, R. Sadat, D. Baleanu, Dynamics of multi-point singular fifth-order Lane–Emden system with neuro-evolution heuristics, Evolving Systems (2022) 1–12.
[47] Z. Sabir, M.R. Ali, M.A.Z. Raja, M. Shoaib, R.A.S. Núñez, R. Sadat, Computational intelligence approach using Levenberg–Marquardt backpropagation neural networks to solve the fourth-order nonlinear system of Emden–Fowler model, Eng. Comput. (2021) 1–17.
[48] Y. Guerrero–Sánchez, et al., Solving a Class of Biological HIV Infection Model of Latently Infected Cells Using Heuristic Approach, Discrete & Continuous Dynamical Systems-S, 2020.
[49] D.Y. Trejos, J.C. Valverde, E. Venturino, Dynamics of infectious diseases: a review of the main biological aspects and their mathematical translation, Applied Mathematics and Nonlinear Sciences 7 (1) (2022) 1–26.
[50] A. Ayub, et al., Characteristics of Melting Heat Transport of Blood with Time-dependent Cross-Nanofluid Model Using Keller–Box and BVP4C Method. Engineering with Computers, 2021, pp. 1–15.
[51] N.A. Shah, P. Agarwal, J.D. Chung, E.R. El-Zahar, Y.S. Hamed, Analysis of optical solitons for nonlinear Schrödinger equation with detuning term by iterative transform method, Symmetry 12 (11) (2020) 1850.
[52] P. Agarwal, A. Berdyshev, E. Karimov, Solvability of a non-local problem with integral transmitting condition for mixed type equation with Caputo fractional derivative, Results Math. 71 (3–4) (2017) 1235–1257.
[53] P. Trikha, E.E. Mahmoud, L.S. Jahanzaib, R.T. Matoog, M. Abdel-Aty, Fractional order biological snap oscillator: analysis and control, Chaos, Solit. Fractals 145 (2021), 110763.
[54] S. Althubiti, M. Kumar, P. Goswami, K. Kumar, Artificial neural network for solving the nonlinear singular fractional differential equations, Applied Mathematics in Science and Engineering 31 (1) (2023), 2187389.
[55] R.T. Matoog, A.H. Salas, R.A. Alharbey, S.A. El-Tantawy, Rational solutions to the cylindrical nonlinear Schrödinger equation: Rogue waves, breathers, and Jacobi breathers solutions, J. Ocean Eng. Sci. 13 (2022) 19.
[56] E. Hou, A. Hussain, A. Rehman, D. Baleanu, S. Nadeem, R.T. Matoog, I. Khan, E.S.M. Sherif, Entropy generation and induced magnetic field in pseudoplastic nanofluid flow near a stagnant point, Sci. Rep. 11 (1) (2021), 23736.